Electrostatic Interactions of Colloidal Particles in Nonpolar Solvents: Role of Surface Chemistry and Charge Control Agents†

Sunil K. Sainis, Vincent Germain,‡ Cecile O. Mejean, and Eric R. Dufresne*

Departments of Mechanical Engineering, Chemical Engineering, and Physics, Yale University, New Haven, Connecticut 06511

Received August 7, 2007. In Final Form: October 9, 2007

We study the electrostatic and hydrodynamic interactions of colloidal particles in nonpolar solvents. Using blinking optical tweezers, we can extract the screening length, κ^{-1}, the effective surface potential, $|e\zeta^*|$, and the hydrodynamic radius, a_h, in a single measurement. We apply this technique to suspensions of polystyrene and poly(methyl methacrylate) particles in hexadecane with soluble charge control agents, aerosol sodium di-2-ethylhexylsulfosuccinate (AOT) and polyisobutylene succinimide (OLOA-1200). We find that the electrostatic interactions of these particles depend sensitively on surface composition as well as on the concentration and chemistry of the charge control agent.

1. Introduction

Charge separation is energetically expensive in environments with low dielectric polarizabilities. This high energy cost inhibits ionization in nonpolar solvents ($\epsilon \approx 2$). Nevertheless, charging of colloidal particles has been observed in nonpolar solvents under the influence of various charge control agents.[1] A number of interesting applications have been found for this surprising phenomena. Nonpolar colloids have been used as electrophoretic ink in flexible electronic displays.[2] OLOA, a commercial dispersant, has long been known to charge carbon black in oil,[3] but it is not clear whether electrostatic interactions significantly contribute to its efficacy. Similarly, aerosol-OT has been found to mediate charging in nonpolar environments.[4−7]

Charge control agents affect interparticle interactions and thus influence the stability and electrokinetic properties of nonpolar suspensions. In general, the electrostatic interaction between colloidal particles depends on ζ, the surface potential, and κ^{-1}, the screening length of the solvent. The screening length depends on the concentration and valence of the ionic species in the solvent. When the ion sizes and valences are known, the screening length can be determined from the bulk conductivity. While this electrokinetic approach works well in aqueous systems where the ionic species are well characterized, it fails in many nonpolar environments because neither the valence of the bulk ions nor their hydrodynamic radii are known *a priori*. Thus, the screening length cannot be inferred from the conductivity alone. Alternatively, Prieve et al. have recently demonstrated that time-dependent current response to a stepwise increase in the voltage contains sufficient information to determine the screening length.[8] If the screening length is known, then the surface potential can be determined from the electrophoretic mobility.[9] However, this is doubly challenging. Not only is the screening length difficult to determine, but the electrophoretic mobility of particles in nonpolar solvents is often too low to be measured accurately in conventional electrophoresis setups. Thus, new methods are required to characterize the electrostatic behavior of nonpolar suspensions.

At a deeper level, there is considerable debate on the nature of electrostatic interactions in nonpolar environments. Some observations suggest that the functional form of the interaction between these charged colloidal particles in nonpolar solvents[6,7] is identical to the predictions from the Derjaguin−Landau−Verwey−Overbeek (DLVO) theory[10,11] developed for aqueous enivronments, while others suggest that a counterion-only double-layer theory is needed to describe observed forces.[12] While the surface forces apparatus and atomic force microscope are well suited to measuring forces between macroscopic surfaces or between a particle and a surface,[4,5] they are not appropriate for studying the interactions of free colloidal particles. In an earlier paper, we demonstrated that the equilibrium structure of a nonpolar dispersion can be used to determine interaction potentials.[13,6] Unfortunately, this elegant method is limited to relatively weak interactions of monodisperse particles with pairwise additive interactions.

In this paper, we extract interparticle forces from the statistics of trajectories of isolated particle-pairs driven out of equilibrium with blinking optical tweezers.[14] We examine the forces between polystyrene (PS) and poly(methyl methacrylate) (PMMA) particles suspended in hexadecane in the presence of charge control agents (aerosol-OT and OLOA-1200). Our recently described method of data analysis[7] self-consistently accounts for the hydrodynamic interactions and yields the solvent screening length, the apparent particle surface potential, and the particle hydrodynamic radius, a_h, in a single measurement. We find that the composition and concentration of the charge control agent have a significant impact on the apparent surface potential and screening length. Similarly, we observe significant differences in surface potential due to changes in surface functionalization.

† Part of the Molecular and Surface Forces special issue.

‡ Present address: Laboratoire des Multimatériaux et Interfaces, UMR CNRS 5615, Université Lyon I, Villeurbanne Cedex, France.

(1) Morrison, I. D. *Colloids Surf., A* **1993**, *71*, 1.
(2) Comiskey, B.; Albert, J. D.; Yoshizawa, H.; Jacobson, J. *Nature* **1998**, *394*, 253.
(3) Pugh, R. J.; Matsunaga, T.; Fowkes, F. M. *Colloids Surf.* **1983**, *7*, 183.
(4) Briscoe, W. H.; Horn, R. G. *Langmuir* **2002**, *18*, 3945.
(5) McNamee, C. E.; Tsujii, Y.; Matsumoto, M. *Langmuir* **2004**, *20*, 1791.
(6) Hsu, M.; Dufresne, E. R.; Weitz, D. A. *Langmuir* **2005**, *21*, 4881.
(7) Sainis, S. K.; Germain, V.; Dufresne, E. R. *Phys. Rev. Lett.* **2007**, *99*, 018303.
(8) Prieve, D. C.; Fu, R. Unpublished data.
(9) O'Brien, R. W.; White, L. R. *J. Chem. Soc., Faraday Trans. 2* **1978**, *74*, 1607.
(10) Derjaguin, B. V.; Landau, L. *Acta Physicochim. URSS* **1941**, *14*, 633.
(11) Verwey, E. J. W.; Overbeek, J. T. G. *Theory of the Stability of Lyophobic Colloids: The Interactions of Sol Particles Having an Electric Double Layer*; Elsevier: New York, 1948.
(12) Briscoe, W. H.; Attard, P. *J. Chem. Phys.* **2002**, *117*, 5452.
(13) Behrens, S. H.; Grier, D. G. *Phys. Rev. E* **2001**, *64*, 050401(R).
(14) Crocker, J. C.; Grier, D. G. *Phys. Rev. Lett.* **1994**, *73*, 352.

10.1021/la702432u CCC: $40.75
Published on Web 12/07/2007

2. Materials

2.1. Colloidal Particles. We report interparticle forces for three types of colloidal particles. We use 1.2 μm PMMA particles with a layer of poly(hydroxystearic acid) (PHSA) stabilizer from Andrew Schofield.[15] We use 1.2 μm diameter carboxylate-modified polystyrene latex (PS-CML) and 1.1 μm diameter amine-modified polystyrene latex (PS-AML) from Interfacial Dynamics Corporation. While PMMA particles are synthesized and shipped in low-dielectric constant solvents, PS particles arrive in aqueous solutions. We transfer these particles to hexadecane through a multistage solvent swap using ethanol as the intermediate solvent. Before the solvent swap, we measured the electrophoretic mobilities of the PS particles in 1 mM NaCl using phase analysis light scattering (Brookhaven ZetaPALS). Using the Smoluchowski relation, we calculated the corresponding zeta potentials: $e\zeta/kT = -3.5 \pm 0.1$ and -1.4 ± 0.1 for the PS-CML and PS-AML particles, respectively. In all cases, very dilute suspensions of these particles ($\phi = 10^{-6}$) are loaded into our sample cell for force measurements.

2.2. Charge Control Agents. We study colloids dispersed in hexadecane with either aerosol-OT (AOT, or sodium di-2-ethylhexylsulfosuccinate) or OLOA-1200 (OLOA, or polyisobutylene succinimide) as charge control agents.

AOT is a surfactant with a sulfonate group on its polar head and two branched hydrocarbon tails. We determined the critical micellar concentration (CMC) to be a few micromoles in hexadecane from conductivity measurements. Above the CMC, AOT forms nanometer-sized reverse-micelles containing about 30 surfactant molecules.[16] AOT reverse micelles can be very hygroscopic, and ambient moisture can affect micelle size. The amount of water absorbed is related to the length of the hydrocarbon solvent. We chose hexadecane as a solvent because it shows a minimal amount of water absorption.[17] To further limit water absorption, we prepare and store our samples in a dry glovebox. We make no attempt to remove water that is in the reagents as received from the manufacturers.

OLOA is a surfactant comprising a succinimide group with long butene chains of variable length. OLOA is used as a steric stabilizer and charge control agent in several applications.[1]

2.3. Sample Cells. Our sample cells are fashioned out of three microscope coverslips on a standard microscope slide as shown in Figure 1a. A standard 25 mm $\times$ 75 mm microscope slide is used as the base of our channel. Two no. 1.5 microscope coverslips are cut and used as spacers to create a pinched channel $\sim$150 μm thick. The top of the channel is sealed using the third coverslip. The pinched channel geometry exploits surface tension to keep the sample pinned in the center of the channel. In some sample cells, the coverslips and the microscope slide are spin-coated with a 200$-$300 nm layer of poly(methyl methacrylate)/poly(methacrylic acid) copolymer (PMMA-MAA), as indicated in Table 1. This coating helps to prevent the adsorption of PMMA spheres to the channel walls. The shallow depth of the channel suppresses convection. The glass surfaces are glued to each other using UV cured epoxy (Norland N61). We cure the epoxy using an intense table top UV source (UV Cure MX). We bake the cells in an oven at 50 °C for 12 h to further set the epoxy. The ends of the channel are left open after the sample is loaded into it.

3. Methods

3.1. Optical Microscopy and Micromanipulation. We image our samples in brightfield with an inverted optical microscope (Nikon TE2000). Images are recorded with a high-speed digital video camera (Photron Fastcam 1024PCI) at a frame rate from 250 to 500 Hz. Images are magnified 150$-$375 times via the objective lens (100$\times$, 1.4 N.A.) and relay optics.

We manipulate particles using holographic optical tweezers. For tweezing experiments in our AOT/hexadecane system, the 532 nm output of a diode-pumped solid-state laser (Coherent Verdi V-5) is

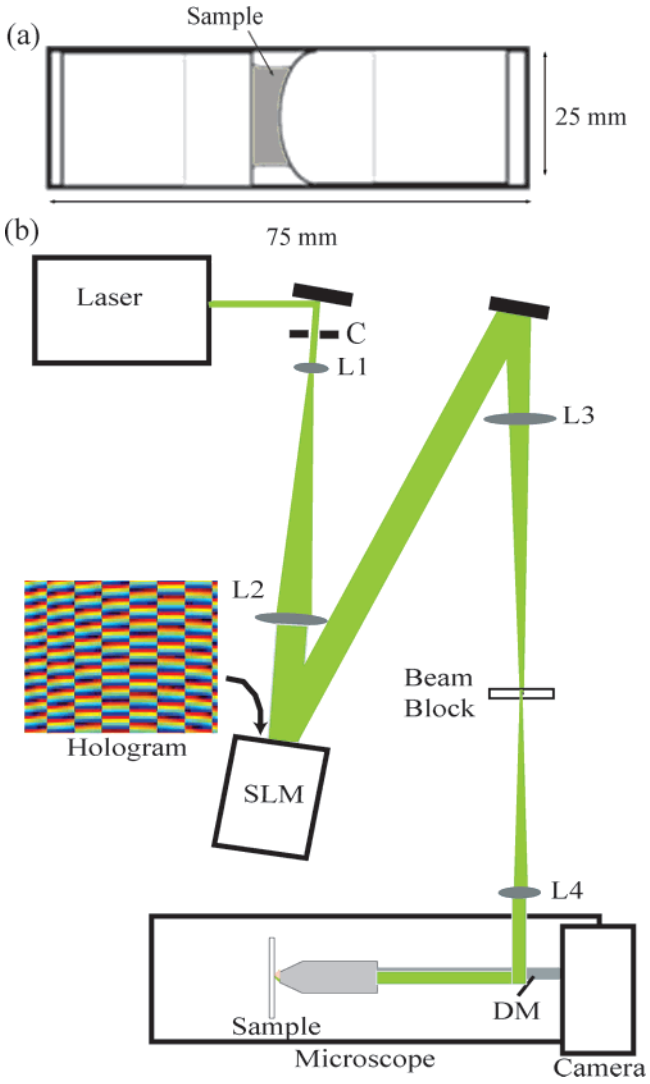

Figure 1. (a) Schematic of the sample cell used in our experiment. (b) Schematic of our optical microscopy and micromanipulation system.

expanded via a Keplerian telescope (L1, L2) to fill the face of a spatial light modulator (SLM; Holoeye LC-R-2500). The SLM modifies the phase of the laser wavefront in the input plane of the microscope objective lens to control the geometry and intensity of the traps near the focal plane.[18$-$20] A typical phase mask is shown alongside the SLM in Figure 1. A detailed discussion of the control system used in these experiments can be found in a recent article.[21] A second Keplerian telescope (L3, L4) projects a demagnified image of the SLM onto the back focal plane of the microscope objective. A ball bearing in the telescope's intermediate focal plane removes the SLM's zeroth-order spot. The laser light is coupled into the microscope objective using a dichroic mirror (DM; Chroma Technology). The trap laser light is blinked using a chopper (C; Thorlabs MC1000A) at 20 Hz.

As our OLOA/hexadecane samples absorb significant amounts of 532 nm light, we study these samples with a separate near-infrared tweezing setup. This setup for the 1064 nm light is identical to our previous construction with the following exceptions: we use a 1064 nm laser (Coherent Compass 1064) and a spatial light modulator (SLM; Holoeye HEO-1080), and all our optics are coated to ensure high efficiency at this frequency.

(15) Antl, L.; Goodwin, J. W.; Hill, R. D.; Ottewil, R. H.; Owens, S. M.; Papworth, S. *Colloids Surf.* **1986**, *17*, 67.
(16) Mathews, M. B.; Hirschhorn, E. *J. Colloid Sci.* **1953**, *8*, 89.
(17) Hou, M.-J.; Shah, D. O. *Langmuir* **1987**, *3*, 1086.
(18) Dufresne, E. R.; Grier, D. G. *Rev. Sci. Instrum.* **1998**, *69*, 1974.
(19) Dufresne, E. R.; Spalding, G. C.; Dearing, M. T.; Sheets, S. A.; Grier, D. G. *Rev. Sci. Instrum.* **2001**, *72*, 1810.
(20) Liesener, J.; Reicherter, M.; Haist, T.; Tiziani, H. J. *Opt. Commun.* **2000**, *185*, 77.
(21) Chapin, S. C.; Germain, V.; Dufresne, E. R. *Opt. Express* **2006**, *14*, 13095.

Table 1. Values of κ^{-1} and $e\zeta^*/k_BT$ Inferred from Various Measurements[a]

type	a [nm]	[AOT]	[OLOA]	κ^{-1} [μm]	$\lvert e\zeta^*/k_BT\rvert$	a_h [nm]	Z^*
CML	600	1 mM		5 ± 1	3.30 ± 0.04	573 ± 9	79 ± 2
CML	600	10 mM		0.6 ± 0.1	1.8 ± 0.1	600 ± 10	71 ± 6
AML	550	1 mM		5 ± 2	1.84 ± 0.06	498 ± 8	36 ± 2
AML	550	10 mM		0.6 ± 0.3	2.6 ± 1.5	499 ± 9	83 ± 47
PMMA[b]	600	1 mM		9 ± 3	2.72 ± 0.07	584 ± 7	62 ± 8
PMMA[b]	600	10 mM		1.4 ± 0.2	2.42 ± 0.06	597 ± 8	74 ± 4
PMMA	600		0.1% w/w			610 ± 10	
PMMA	600		1.0% w/w			534 ± 7	

[a] a is the nominal radius of the beads as reported by the supplier. [b] b denotes measurements where the sample cell was coated with a layer of PMMA-MAA.

3.2. Force Measurement. We extract interparticle forces from the statistical properties of the trajectories of isolated pairs of beads. As described in greater detail elsewhere,[7] we repeatedly trap and release beads with blinking optical tweezers to thoroughly sample the stochastic dynamics of freely interacting particles. Provided that gradients in hydrodynamic coupling are not too strong, the short-time dynamics of particle trajectories are well-characterized by two kinematic parameters: the mean drift velocity, v, and the diffusion coefficient, D. These two quantities are related to the interparticle force, F, through a generalization of the Stokes−Einstein relation:

$$F = k_B T \frac{v}{D} \tag{1}$$

Thus, the spatial dependence of the kinematic parameters, $v(r)$ and $D(r)$, provide the interparticle force, $F(r)$.

4. Results and Discussion

Typical data showing the spatially resolved relative diffusion coefficient, $D(r)$, and the velocity of separation, $v(r)$, are shown in Figure 2. At large separations, where particles do not interact, the diffusion coefficient tends toward its Stokes−Einstein value and the drift velocity goes to zero. At smaller separations, hydrodynamic and electrostatic interactions become evident. Viscous coupling between the spheres suppresses relative motion at small separations. This leads to a monotonically decreasing diffusion coefficient, $D(r)$, as the particles approach each other, as shown in Figure 2a. This coupling is well-captured by a first order correction to the hydrodynamic mobility[22,23] as given by

$$D(r) = 2D_0\left(1 - \frac{3}{2}\frac{a_h}{r}\right) \tag{2}$$

Here, D_0 is the self-diffusion coefficient,

$$D_0 = \frac{k_B T}{6\pi\eta a_h} \tag{3}$$

where η is the viscosity of the solvent. In our samples, η varies negligibly with the concentration of charge control agent used. For the most part, the values of a_h returned by our fits (see Table 1) lie within the polydispersity limits reported by the particle manufacturers. Interestingly, we consistently observe a slight increase in the hydrodynamic radii with increasing AOT concentration. This may be a subtle signature of the adsorption of reverse micelles onto the particle surface.

Electrostatic forces drive a significant drift of particles away from each other at smaller separations, as shown in Figure 2b. The magnitude of this drift velocity is determined by a competition of electrostatic repulsions and viscous drag. We extract the underlying forces by comparing the relative magnitudes of drift and diffusion, as quantified in eq 1. An illustrative collection of force profiles acquired in this fashion are plotted in Figures 3−5. We typically measure a relatively large force (≈100 fN) at small separations ($r \approx 2$ μm) that decays to a value less than our resolution (≈5 fN) over several particle radii. All interaction curves are surprisingly well fit by a conventional screened-Coulomb form,

$$F(r) = k_B T\left(\frac{e\zeta^*}{k_B T}\right)^2 \frac{a^2}{\lambda_B}\frac{e^{-\kappa(r-2a)}}{r}\left[\frac{1}{r} + \kappa\right] \tag{4}$$

where the Bjerrum length, $\lambda_B = e^2/4\pi\epsilon\epsilon_0 k_B T$, characterizes the dielectric polarizability of the solvent. These fits return screening lengths, κ^{-1}, and effective surface potentials, $|e\zeta^*|$, assuming a nominal particle radius, as given by the manufacturers. Using the measured hydrodynamic radii in these fits does not

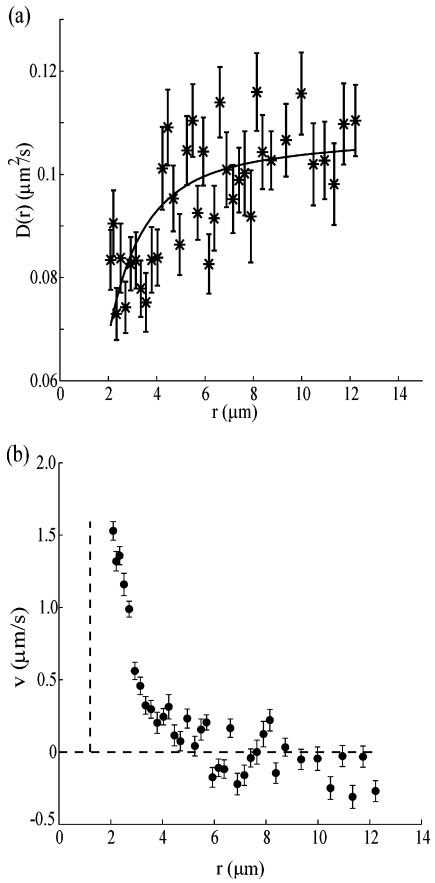

Figure 2. Separation dependence of the relative diffusion coefficient, D, and relative velocity, v. Error bars indicate estimated one σ confidence intervals from the linear fits to the mean and variance of particle displacements over time. These data were taken with PMMA-PHSA beads ($a = 600$ nm) in a 10 mM AOT/hexadecane mixture at a chopper rate of 20 Hz and a frame rate of 500 fps.

(22) Batchelor, G. K. *J. Fluid. Mech.* **1976**, *74*, 1.
(23) Dufresne, E. R.; Squires, T. M.; Brenner, M. P.; Grier, D. G. *Phys. Rev. Lett.* **2000**, *85*, 3317.

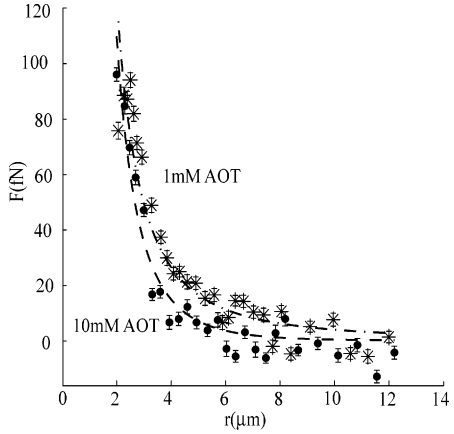

Figure 3. Dependence of the interactions of two isolated PMMA-PHSA beads ($a \approx 600$ nm) on the concentration of AOT. Curves are fits to the screened-Coulomb interaction.

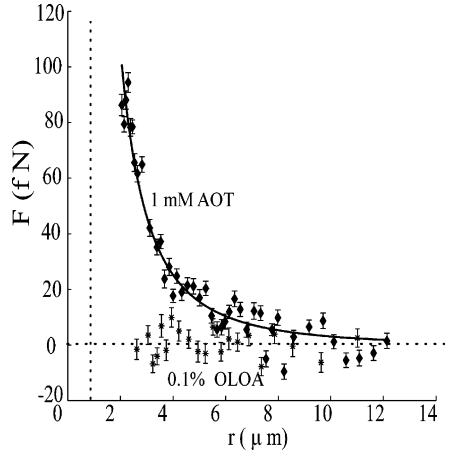

Figure 4. Dependence of the force between two isolated PMMA beads ($a \approx 600$ nm) on the charge control agent.

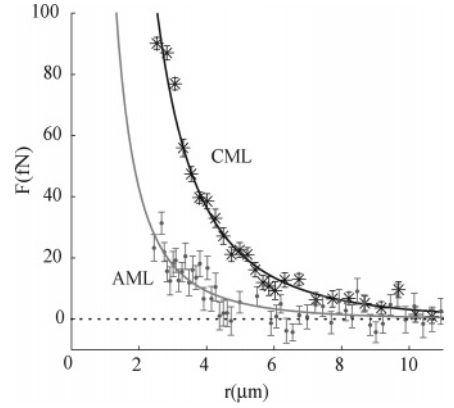

Figure 5. Surface chemistry dependence of the interaction force. Comparison of the interaction force between isolated pairs of CML beads and the interaction force between AML beads at 1 mM AOT. Both curves are fits to the screened-Coulomb interaction.

significantly change fitting parameters. We present a complete set of fitting parameters in Table 1.

The concentration of AOT affects both the screening length and the effective surface potential, as shown in Figure 3. Here, we display the interaction forces for isolated pairs of PMMA-PHSA beads in 1 and 10 mM AOT/hexadecane solutions.

At 1 mM AOT, the effective surface potential is relatively large, $|e\zeta^*/k_BT| = 2.72 \pm 0.07$, and the screening length is much larger than the particle diameter, $\kappa^{-1} = 9 \pm 3$ μm. At 10 mM AOT, the effective surface potential is slightly lower, $|e\zeta^*/k_BT| = 2.42 \pm 0.06$, while the screening length becomes comparable to the particle diameter, $\kappa^{-1} = 1.4 \pm 0.2$ μm. It is important to note that fitted values of $|e\zeta^*|$ reflect the effective surface potential as seen from long-range. This value will be smaller than the actual surface potential, $|e\zeta|$, for highly charged surfaces due to nonlinear screening near the particle surface. Combining these results, we can now estimate the particle charge, Z^*:[24]

$$Z^* = \frac{a(1+\kappa a)}{\lambda_B}\left|\frac{e\zeta^*}{k_BT}\right| \tag{5}$$

Using this expression, which is only strictly valid for $|e\zeta^*/k_BT| \ll 1$, we find a particle charge of 62 ± 8 and 74 ± 4 for the 1 and 10 mM samples, respectively. It is interesting to note that while these nonpolar colloids exhibit effective surface potentials comparable to those found in highly charged aqueous systems, their screening lengths are much larger and their surface charge densities are much lower than their aqueous counterparts. Pair potentials of a closely related system (PMMA-PHSA in AOT/dodecane) were extracted from the equilibrium structure of suspensions by Hsu et al.[6] They found similar values of effective surface potential and screening length. That article identified the thermal ionization of AOT reverse micelles as the source of bulk ions and demonstrated the coupling of effective surface potential to ionic strength.

Charge control agents must be carefully matched to particle surface chemistry. Stimulated by various reports of charging induced by OLOA, we compared the interaction between identical PMMA-PHSA beads suspended in either AOT/hexadecane or OLOA/hexadecane. As seen in Figure 4, AOT is considerably more effective than OLOA at charging PMMA beads in hexadecane. Measurements at 0.1% w/w and 1% w/w OLOA show no interparticle repulsion above the noise level of our measurement and therefore no evidence of surface charging. Since OLOA absorbs strongly in the visible spectrum, these measurements were performed on a near-infrared optical trapping system. While particles were trappable with 1064 nm light, there was some residual absorption at this wavelength. This absorption may have led to local heating which lowered the apparent hydrodynamic radius by about 10%. A measurement of the temperature dependence of the viscosity of hexadecane (TA AR-2000 rheometer) shows that a temperature increase of 10 °C could account for this difference.

Surface functionalization also has a strong effect on particle interactions. To isolate the effect of surface chemistry, we compared the interactions of amine modified PS latex beads (AML; $a \approx 550$ nm) and carboxyl modified PS latex beads (CML; $a \approx 600$ nm) suspended in identical solvents (1 and 10 mM AOT/hexadecane). Results for 1 mM AOT are shown in Figure 5. In these conditions, we find that electrostatic repulsions between carboxylated spheres are much stronger than those of aminated spheres, $\zeta^*_{CML}/\zeta^*_{AML} = 3.3/1.8$. Interestingly, this trend is also observed in electrokinetic measurements on the same spheres in water, $\zeta_{CML}/\zeta_{AML} = 3.5/1.4$. Reassuringly, the measured values of the screening length for the two particle types agree well for identical concentrations of AOT, as shown Table 1.

Since the screening length is a property of the solvent, it should not vary with particle surface chemistry. Results for 10 mM AOT also show good agreement of the screening lengths for the two types of particles, but the large error bars on $|\zeta^*|$ in the AML data set do not allow for meaningful comparisons between the two surface chemistries.

(24) Trizac, E.; Bocquet, L.; Aubuoy, M. *Phys. Rev. Lett.* **2002**, *89*, 2002.

One anomalous feature of our data presented in Table 1 is the disagreement in the screening length measured for PS and PMMA spheres at identical concentrations of AOT. We suspect that this deviation is caused by two factors. First, PS measurements were conducted on the same humid summer day and the PMMA measurements were done a few months later on a relatively dry fall day. Thus, there could more water in the PS samples than the PMMA samples. Using conductivity measurements, we have independently confirmed variations in the ionic strength with ambient humidity. Second, PS measurements were conducted in bare glass sample chambers while PMMA measurements were conducted in PMMA-MAA-coated glass sample chambers. This difference may have shifted the equilibrium of surfactant adsorption to lower the effective concentration of AOT in the sample chamber.

5. Conclusions

Our measurements of interparticle forces in nonpolar colloids reveal long-range electrostatic interactions that are tunable by surface functionalization and soluble charge control agents. While the effective surface potentials are comparable to those observed in aqueous systems, the screening lengths in oil are much larger and the charge densities are much lower. These observations are consistent with earlier work.[6,7] We document the first observations of the dependence of electrostatic interactions in nonpolar environments on the chemistries of the particle surface and charge control agent. These results raise a number of intriguing questions regarding the detailed chemical mechanisms of interfacial charging in nonpolar environments. A recent paper by Smith et al. complements this study.[25] They observed the effects of the composition of particle surface and charge control agent on the zeta potential in electrokinetic phenomena. They present detailed chemical mechanisms to rationalize the observed trends.

Acknowledgment. We thank Ian Morrison for helpful discussions. We thank Andrew Schofield for providing the PMMA particles and PHSA stabilizer and Chevron for the sample of OLOA-1200. We would like to thank the Cabot Corporation, the National Institute for Nano Engineering at Sandia National Laboratory, and the National Institutes of Health (1U54-RR022232) for their support.

LA702432U

(25) Smith, P. G.; Patel, M. N.; Kim, J.; Milner, T. E.; Johnston, K. P. *J. Phys. Chem. C* **2007**, *111*, 840.